# Supporting Information

## Tuning the Microenvironment of Immobilized Molecular Catalyst for Selective Electrochemical $CO_2$ Reduction

*Ziying Qin,[a] Haocheng Zhuang,[a] Dayou Song,[a] Gong Zhang,[a] Hui Gao,[a] Xiaowei Du,[a] Mingyang Jiang,[a] Peng Zhang,[*abcdef] and Jinlong Gong[*abcdefg]*

**Corresponding Authors**

**Peng Zhang -** Email: p_zhang@tju.edu.cn; **Jinlong Gong -** Email: jlgong@tju.edu.cn

[a] School of Chemical Engineering & Technology, Key Laboratory for Green Chemical Technology of Ministry of Education, Tianjin University; Collaborative Innovation Center for Chemical Science & Engineering; Tianjin, 300072, China.

[b] Joint School of National University of Singapore and Tianjin University, International Campus of Tianjin University, Binhai New City, Fuzhou 350207, China

[c] International Joint Laboratory of Low-carbon Chemical Engineering of Ministry of Education, Tianjin 300350, China

[d] Haihe Laboratory of Sustainable Chemical Transformations, Tianjin 300192, China

[e] National Industry-Education Platform of Energy Storage, Tianjin University, 135 Yaguan Road, Tianjin, 300350, China

[f] Tianjin Normal University, Tianjin, 300387, China

[g] State Key Laboratory of Synthetic Biology, Tianjin University, Tianjin, 300072, China

## Experimental Section

**Materials.** Cobalt phthalocyanine (CoPc, 95%) was purchased from Shanghai Miner Chemical Technology Co., Ltd. Carbon nanotubes (CNT) and N, N-dimethylformamide (DMF) were bought from J&K China Chemical Co., Ltd. Potassium hydroxide (KOH, 95%) was purchased from Shanghai Aladdin Biochemical Technology Co., Ltd. Polytetrafluoroethylene (PTFE) was bought from Shanghai Macklin Biochemical Co., Ltd. *tert*-Butyl alcohol (*t*-BuOH) was bought from TCI (Shanghai) Development Co., Ltd. Gas diffusion electrode (GDE, Sigracet 39 BC), anion exchange membrane (AEM, Fumasep FAA-3-50), Fumion FAA-3-SOLUT-10 (FAA solution, 25%) was purchased from Fuel Cell Store. 99.999% purity carbon dioxide gas was purchased from Air Liquid. All solutions used ultrapure water (18.25 MΩ·cm) obtained from UP Water Purification System. All chemicals were used as is, without further purification.

**Synthesis of CoPc/CNT, PTFE-CoPc/CNT and AD-PTFE-CoPc/CNT.** *Pretreatment of CNT.* For the pretreatment, CNTs were subjected to a 24-hour treatment in 1.0 M HCl to remove metallic impurities. To activate the surface, CNTs were mixed with nitric acid (69 wt%) and heated at 60 °C for 2 hours. The resultant CNTs were washed with deionized water until reaching a neutral pH and subsequently dried at 80 °C.

*Synthesis of CoPc/CNT.* In a typical synthesis of CoPc/CNT, a general modified impregnation method was employed. Specifically, 2 mg of CoPc powder was added to 30 mL of DMF and sonicated for 30 minutes to obtain a homogeneous solution. Subsequently, 30 mg of pre-treated CNT was added to the CoPc/DMF solution, and the mixture was sonicated for an additional 30 minutes. After the impregnation, the mixture was centrifuged at 7000 rpm for 3 minutes to remove the supernatant, and the precipitate was sequentially washed with DMF, deionized water, and ethanol. Finally, the precipitate was dried in an oven at 80 °C.

*Synthesis of PTFE-CoPc/CNT.* A total of 80 mg of pre-treated CNT was spread evenly at the bottom of a beaker. Subsequently, 20 mg of PTFE powder was added to 0.8 mL of *t*-BuOH and sonicated for 5 minutes to form a stable dispersion. Then, this dispersion was added dropwise onto the CNT powder. The beaker was placed on an oscillator to ensure the thorough infiltration of the dispersion into the CNT, resulting in a slurry-like mixture. The obtained slurry-like mixture was then subjected to 10 minutes of ultrasound treatment to achieve a good dispersion of PTFE between the CNT. After impregnation, the mixture was dried overnight in an oven at 80 °C, yielding a gray powder denoted as PTFE-CNT. Subsequently, 30 mg of PTFE-CNT was used to immobilized CoPc on the CNT following the method described in *Synthesis of CoPc/CNT*, resulting in PTFE-CoPc/CNT.

*Synthesis of AD-PTFE-CoPc/CNT.* The PTFE-CNT was obtained using the method described in *Synthesis of PTFE-CoPc/CNT*. The prepared PTFE-CNT was placed in a tube furnace (Hefei KeJing Materials Technology Co., LTD) with flowing $N_2$ at 200 sccm and heated at 400 °C for 2 h. The obtained sample was cooled slowly to room temperature in $N_2$ and referred to as AD-PTFE-CNT. Subsequently, 30 mg of AD-PTFE-CNT was used to immobilized CoPc on the CNT following the method described in *Synthesis of CoPc/CNT*, resulting in AD-PTFE-CoPc/CNT.

*Synthesis of AD-PTFE-CoPc/CNT with 0 wt%, 10 wt%, 20 wt% and 30 wt% PTFE.* A total of 80 mg of pre-treated CNT was spread evenly at the bottom of a beaker. Then, 0 mg, 8.9 mg, 20.0 mg and 34.3 mg of PTFE powder were added to 0.8 mL of *t*-BuOH and sonicated for 5 minutes to form a stable dispersion. Subsequently, PTFE-CNT with 0 wt%, 10 wt%, 20 wt%, and 30 wt% PTFE was obtained following the method described in *Synthesis of PTFE-CoPc/CNT*, and AD-PTFE-CoPc/CNT with 0 wt%, 10 wt%, 20 wt%, and 30 wt% PTFE was synthesized following the method described in *Synthesis of AD-PTFE-CoPc/CNT*.

**Characterization**. X-ray diffraction (XRD) patterns were recorded using a Bruck D8-Focus diffractometer equipped with Cu Kα radiation (λ = 1.5406 Å). Inductively coupled plasma mass spectrometry (ICP-MS) was conducted on an Agilent 7800 to quantify the concentration of cobalt (Co). Scanning electron microscope images (SEM) were obtained by Hitachi S-4800. SEM combined with energy-dispersive X-ray spectroscopy (EDS) was taken to investigate the elemental distribution of the catalysts. The contact angles were measured using a contact angle system (OCA 20, Dataphysics, Germany) at ambient temperature. Cross-section fluorescence images of the electrodes were obtained using a confocal laser scanning microscopy (CLSM) on an N-C2-SIM (Nikon, Japan) CLSM. During CLSM testing, a thin layer of 1M KOH electrolyte containing a fluorescent dye (i.e., 8-hydroxypyrene-1,3,6-trisulfonic acid) was placed in a confocal dish, and a GDE coated with catalyst was positioned upside down over the electrolyte. During the test, a laser positioned below the confocal dish emitted a beam, which sequentially passed through the confocal dish and electrolyte before reaching the GDE. By collecting fluorescence signals emitted by the laser-excited dye, changes at the electrolyte–GDE interface were analyzed to investigate the three-phase interface.

**Electrochemical measurements.** *Preparation of working electrodes.* A total of 10 mg of the sample was mixed with 80 μL of FAA solution in 2 mL of DMF and sonicated for 30 minutes to form an ink solution. For PTFE-ink-CoPc/CNT, 8 mg of CoPc/CNT, 2 mg of PTFE powder, and 80 μL of FAA solution were mixed in 2 mL of DMF and sonicated for 30 minutes to form the ink solution. Then, the solution was deposited onto gas diffusion electrode (GDE) using an airbrush deposition technique, with a sample mass loading of 1 mg/cm$^2$. The GDE was baked during a regular heating stage at a temperature not exceeding 50 °C.

*Electrochemical measurements in a flow cell.* Electrochemical $CO_2$ reduction measurements were performed in a typical three-electrode flow cell reactor at first. The effective electrode geometric area is 1 cm$^2$ for both the cathode and anode. Anolyte and catholyte chambers were

separated by an anion exchange membrane (AEM, Fumasep FAA-3-50). $IrO_x$/Ti was used as the counter electrode and Hg/HgO was used as the reference electrode. The potentials were converted to the RHE reference scale using the relation: E (vs RHE) = E (vs Hg/HgO) + 0.098 V + 0.059 × pH. The 1 M KOH solution was circulated at a flow rate of 15 mL/min using a peristaltic pump. $CO_2$ was delivered into the flow cell at a rate of 10 sccm. The $CO_2$ flow rate at the cathode outlet was measured using a flow meter (M-series, Alicat Scientific). Potentiostat (Cortest CS350M) was employed for applying the current and measuring the cell voltage. Experimental data was collected after the stabilization of the reaction for about 5 minutes.

*Electrochemical measurements in the membrane electrode assembly (MEA) system.* The MEA electrolyzer (Gaossunion Co., Ltd) consists of a GDE cathode with a working area of 4 $cm^2$, an anion exchange membrane (AEM, Fumasep FAA-3-50) and a titanium mesh anode coated with $IrO_2$. It was used for the evaluation of $CO_2$RR performance. The 1 M KOH solution was circulated at a flow rate of 15 mL/min using a peristaltic pump. $CO_2$ was delivered into the MEA system at a rate of 10 sccm. The $CO_2$ flow rate at the cathode outlet was measured using a flow meter (M-series, Alicat Scientific). Cortest CS350M was employed for applying the current and measuring the cell voltage. All reported potentials represent the full-cell potentials without iR compensation. Experimental data was collected after the stabilization of the reaction for about 5 minutes.

*Analysis of $CO_2$RR products*. The gas phase products were delivered to a gas chromatography (GC7890B, Agilent Technologies, Inc.) for on-line analysis. CO and $H_2$ were detected by a flame ionization detector (FID) connected to a Porapak Q packed column and a thermal conductivity detector (TCD) connected to a MolSieve 5A packed column, respectively.

*Calculation of the Faradaic efficiency (FE), CO partial current density ($J_{CO}$) and turnover frequency (TOF)*. The FEs for the different products were calculated based on the moles of

electrons consumed for the formation of various products and the total moles of electrons passed according to the following equation.

$$FE(\%) = \frac{moles\ of\ product\ \times\ number\ of\ e^-\ needed\ for\ conversion}{moles\ of\ e^-\ passed} \times 100\% \quad (1)$$

$$moles\ of\ e^-\ passed\ =\ current\ \times\ time\ /\ Faraday\ constant \quad (2)$$

$$moles\ of\ product\ =\ concentration\ \times\ flow\ rate\ /\ molar\ volume\ \times\ time \quad (3)$$

The formula for calculating the $J_{CO}$ was calculated according to the following equation.

$$J_{CO} = FE_{CO} \times Current\ Density \quad (4)$$

The TOF for CO was calculated according to the following equation.

$$TOF = \frac{J_{CO}/(nF)}{m_{cat} \times w/M_{Co}} \quad (5)$$

Where $J_{CO}$ was partial current (A) for CO product and n stood for the number of electrons transferred for product formation, which was 2 for CO production. As cobalt was the active center, $m_{cat}$ was catalyst mass (g) in the electrode and w was Co loading (%) in the catalyst.

*Calculation of the cell energy efficiency (EE) and the half-cell cathodic energy efficiency (CEE)*. The EE for $CO_2$RR was calculated according to the following equation.

$$EE = \frac{(E_{ox}^0 - E_{CO_2RR}^0) \times FE_{CO}}{E_{ox} - E_{CO_2RR}} \quad (6)$$

Where, $E_{ox}^0$ and $E_{CO_2RR}^0$ are the thermodynamic potentials for water oxidation (1.23 V vs. RHE) and $CO_2$RR to CO (-0.11 V vs. RHE), respectively. $E_{ox}$ and $E_{CO_2RR}$ are the applied potentials at anode and cathode, respectively. For the calculation of the half-cell CEE, the anodic reaction

was assumed to occur with an overpotential of 0 V (that is $^{E_{ox}}$ = 1.23 V).

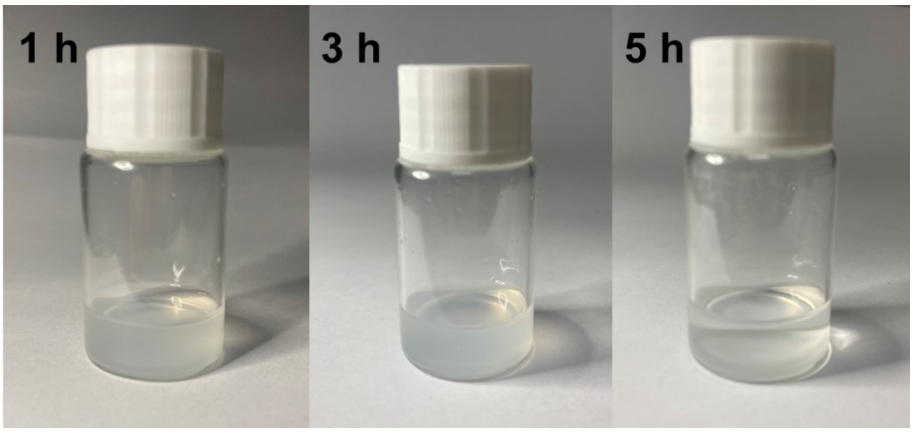


**Figure S1** Photographs of a stable dispersion of PTFE in *t*-BuOH. The dispersion remained stable without any precipitation for 3 hours but exhibited noticeable settling after 5 hours.

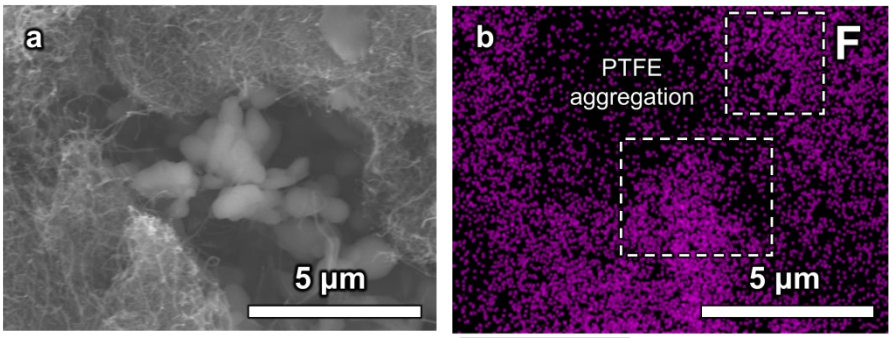


**Figure S2** (a) SEM and (b) EDS elemental mapping images of PTFE-CoPc/CNT. The characteristic fluorine (F) element of PTFE exhibited aggregation.

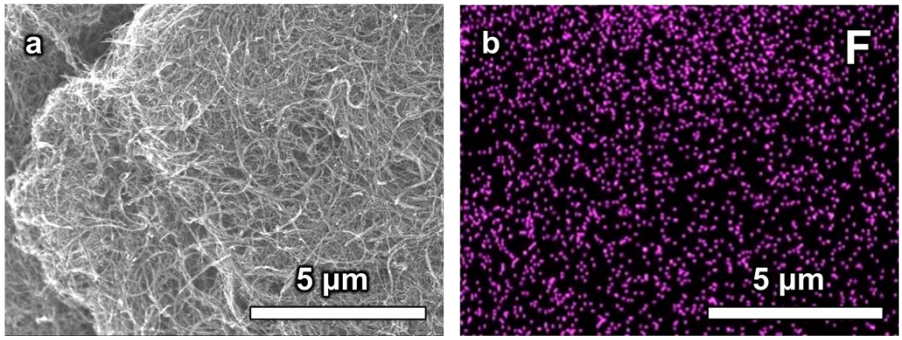


**Figure S3** (a) SEM and (b) EDS elemental mapping images of AD-PTFE-CoPc/CNT. The characteristic fluorine (F) element of PTFE was well-dispersed.

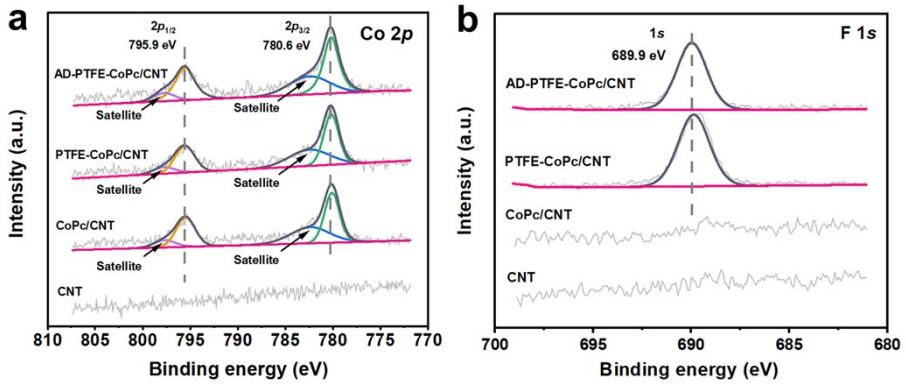


**Figure S4** (a) Co 2p, (b) F 1s XPS spectra of CNT, CoPc/CNT, PTFE- CoPc/CNT and AD-PTFE-CoPc/CNT. The presence or absence of characteristic peak signals indicated the successful modification of Co and F, and no apparent peak shifts observed indicates that the modification by PTFE did not alter the chemical environment.

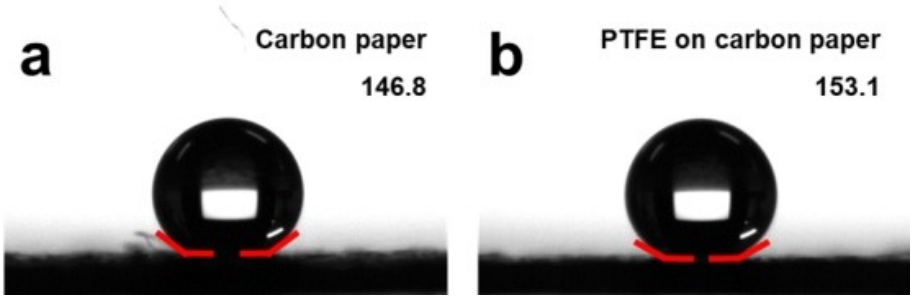


**Figure S5** Contact angles of (a) carbon paper and (b) PTFE on carbon paper with a drop of water.

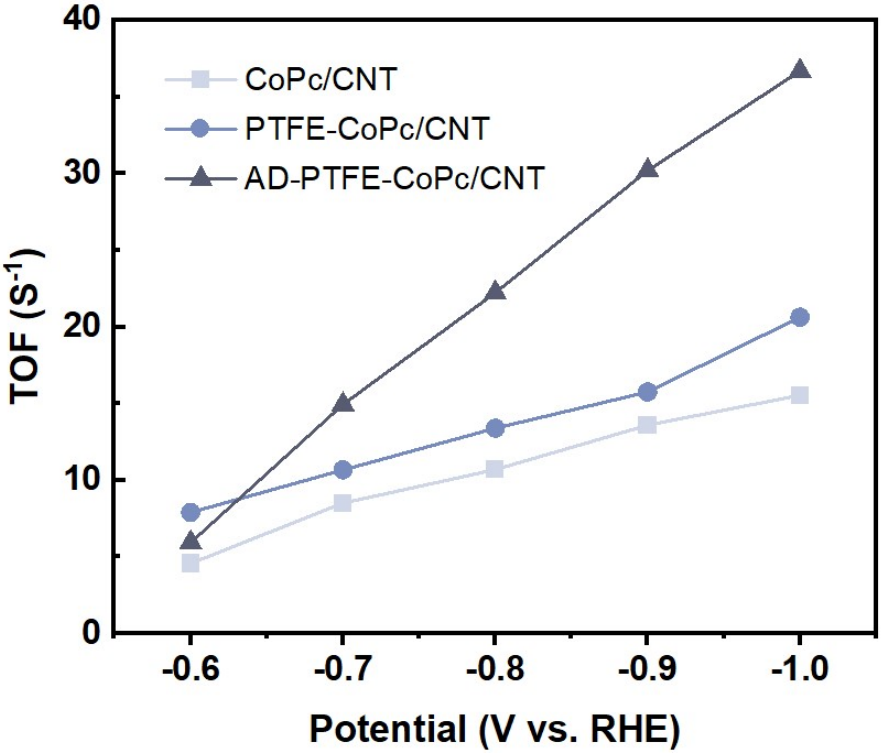


**Figure S6** TOF of $CO_2$RR for CoPc/CNT, PTFE-CoPc/CNT, and AD-PTFE-CoPc/CNT in a flow cell reactor.

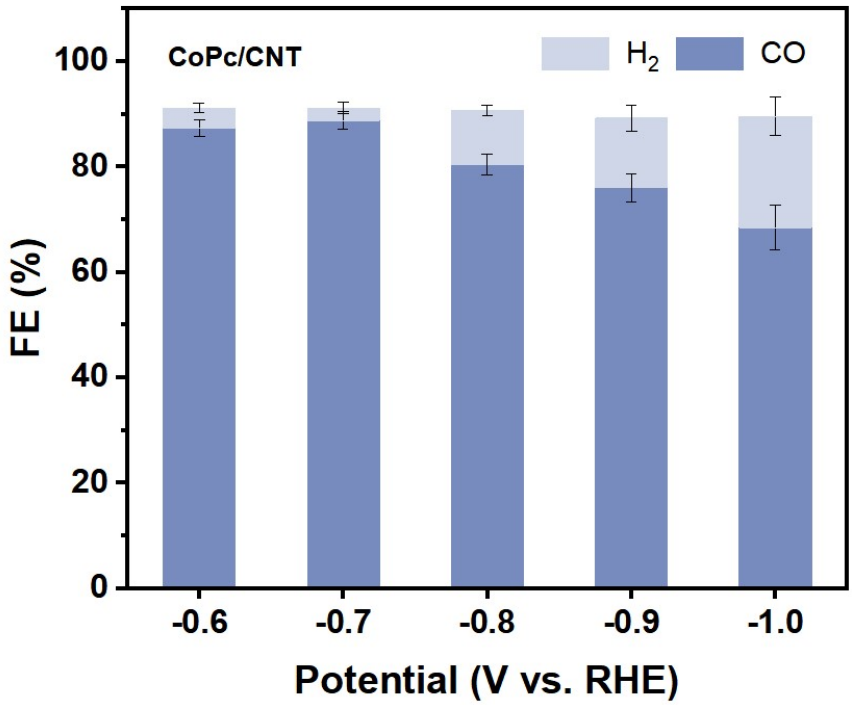


**Figure S7** FE of $CO_2$RR for CoPc/CNT in a flow cell reactor. Starting from -0.8 V, the $FE_{CO}$ of CoPc/CNT fell below 80%.

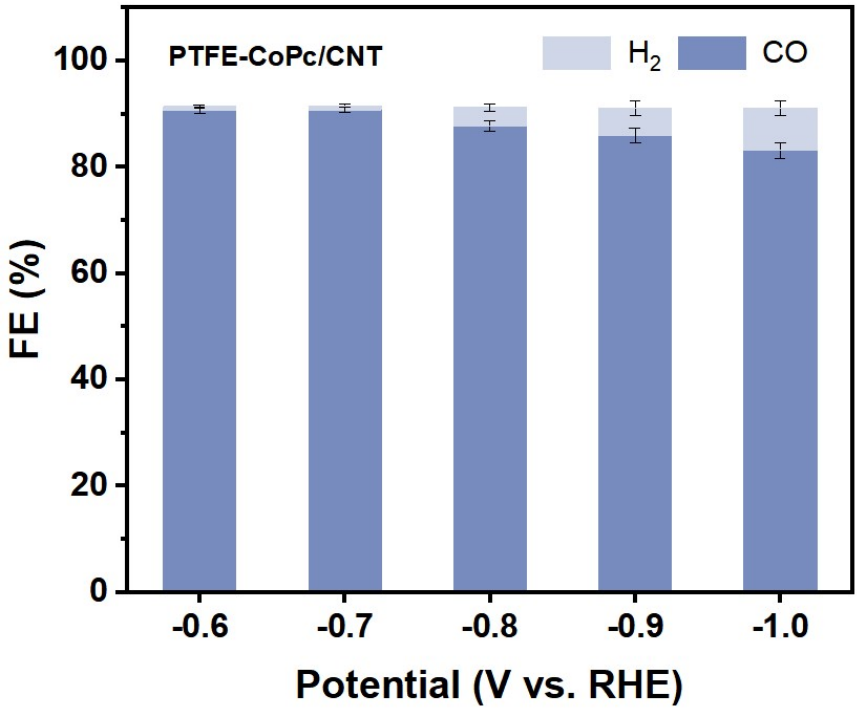


**Figure S8** FE of $CO_2$RR for PTFE-CoPc/CNT in a flow cell reactor.

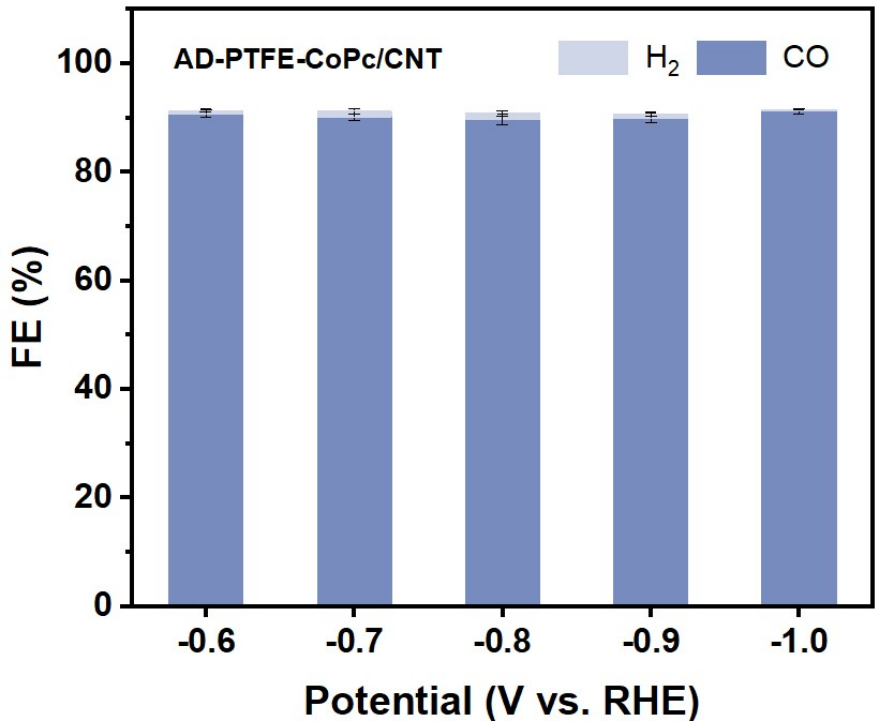


**Figure S9** FE of $CO_2RR$ for AD-PTFE-CoPc/CNT in a flow cell reactor. In the range of -0.6 V to -1.0 V, the FE of AD-PTFE-CoPc/CNT for $H_2$ was less than 1%, while the FE for CO was as high as 90%.

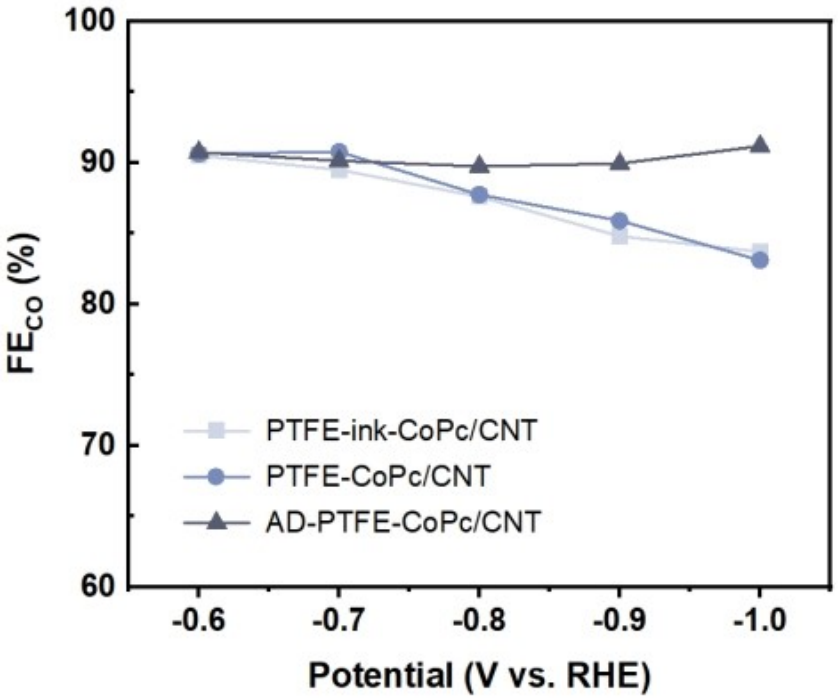


**Figure S10** $FE_{CO}$ of $CO_2RR$ for PTFE-ink-CoPc/CNT, PTFE-CoPc/CNT and AD-PTFE-CoPc/CNT in a flow cell reactor.

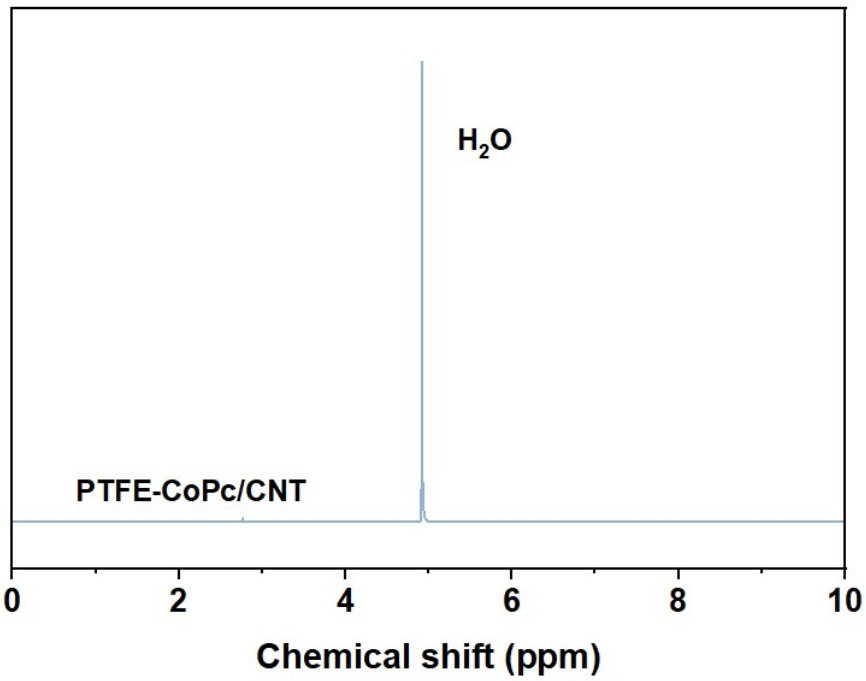


**Figure S11** NMR spectrum of the electrolyte collected from the flow cell reactor in which PTFE-CoPc/CNT was evaluated at -1.0 V, suggesting that there was no liquid product generated from $CO_2$RR.

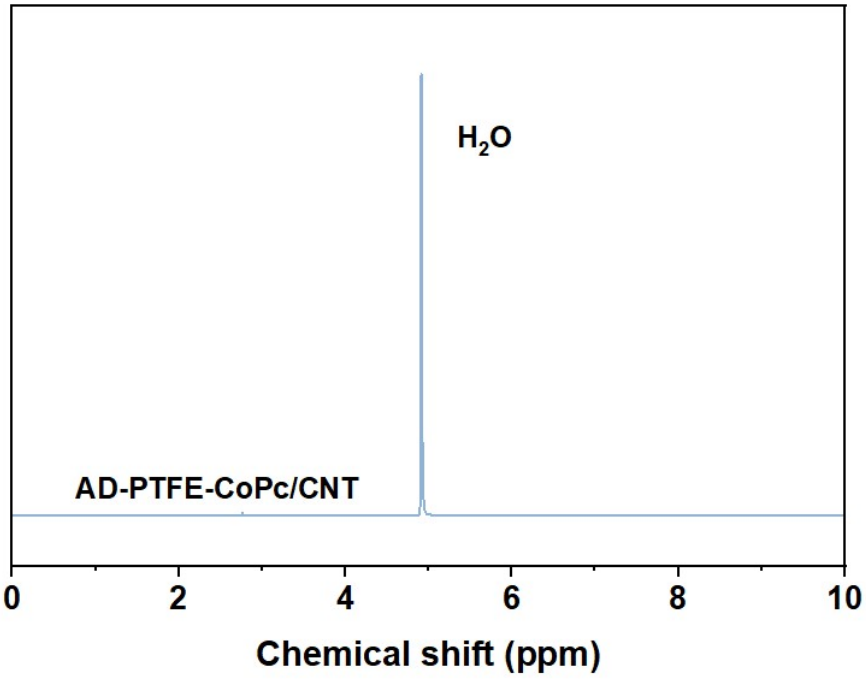


**Figure S12** NMR spectrum of the electrolyte collected from the flow cell reactor in which AD-PTFE-CoPc/CNT was evaluated at -1.0 V, suggesting that there was no liquid product generated from $CO_2$RR.

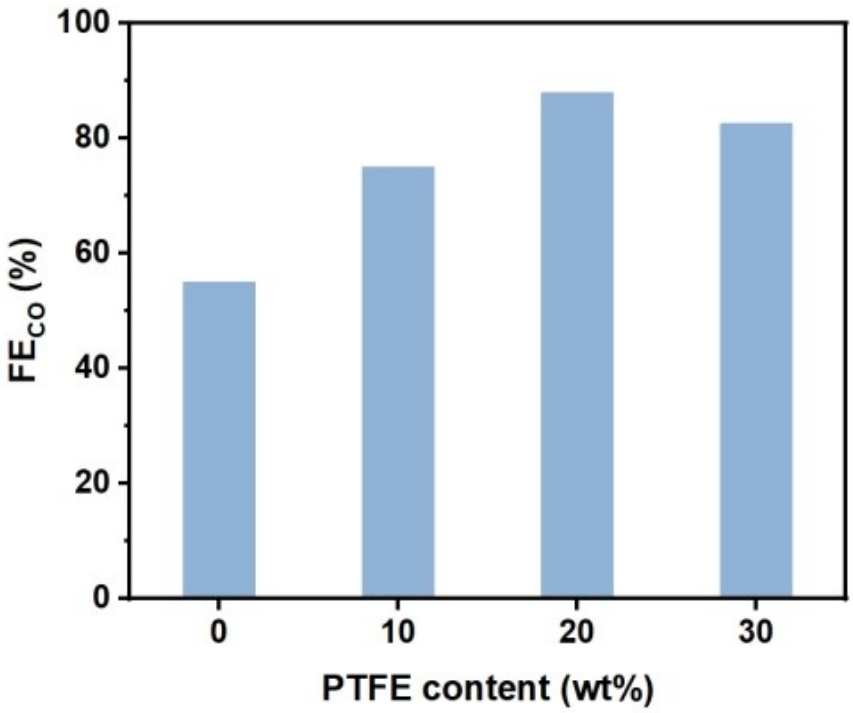


**Figure S13** $FE_{CO}$ of AD-PTFE-CoPc/CNT with 0 wt%, 10 wt%, 20 wt% and 30 wt% PTFE at 100 mA/cm$^2$.

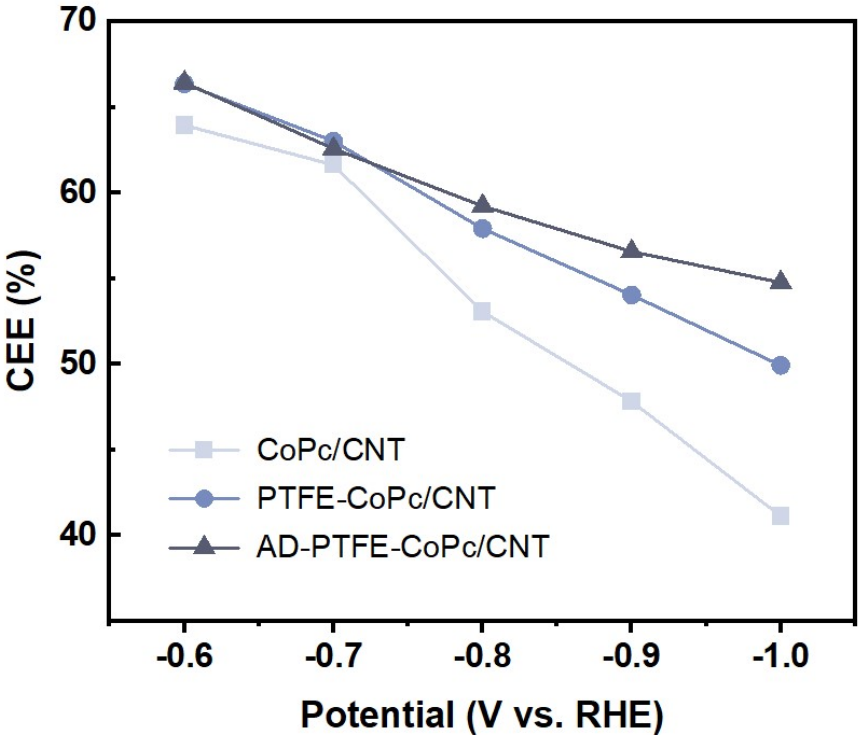


**Figure S14** CEE of CoPc/CNT, PTFE-CoPc/CNT and AD-PTFE-CoPc/CNT.

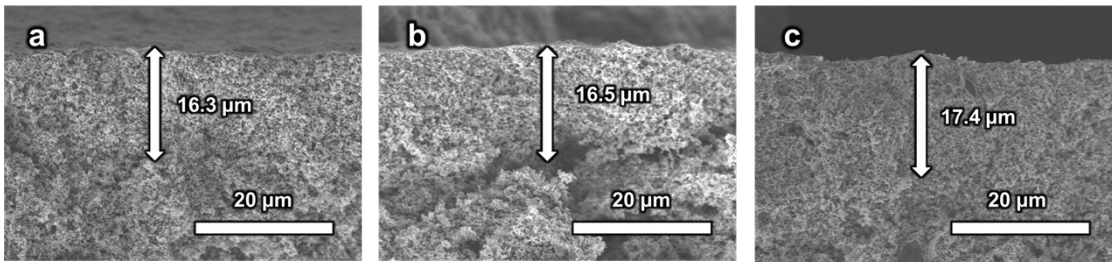


**Figure S15** Cross-sectional SEM image of the electrode after coating with (a) CoPc/CNT, (b) PTFE-CoPc/CNT and (c) AD-PTFE-CoPc/CNT. The thicknesses of catalyst layer were 16.3 µm, 16.5 µm, and 17.4 µm, respectively, with a relatively small difference.

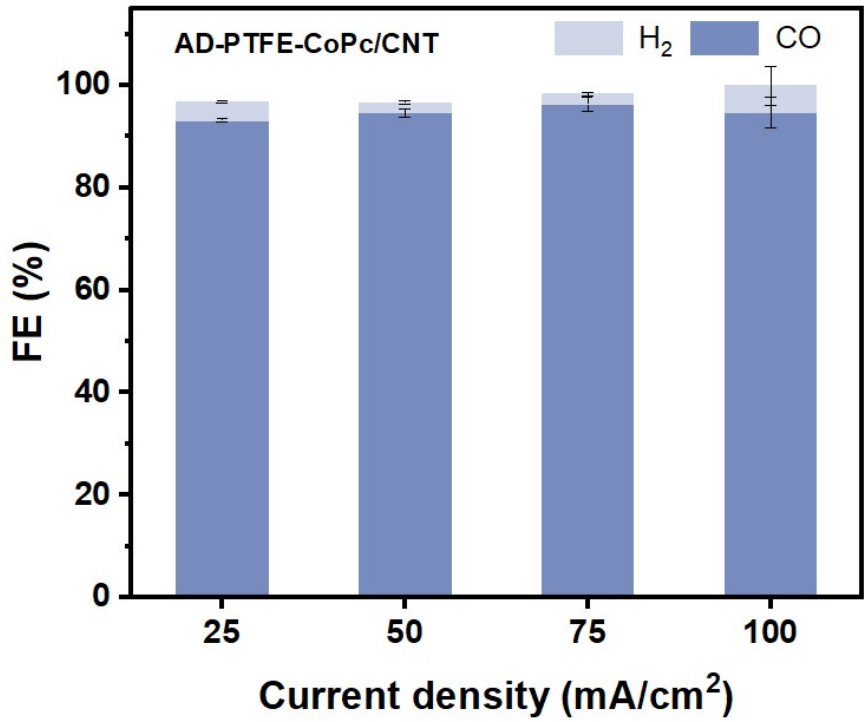


**Figure S16** FE of $CO_2$RR for AD-PTFE-CoPc/CNT in a MEA. AD-PTFE-CoPc/CNT exhibited the best $CO_2$RR performance, with over 90% selectivity for CO in the current range of 0-100 mA/cm$^2$. The overall FEs were around 100%.

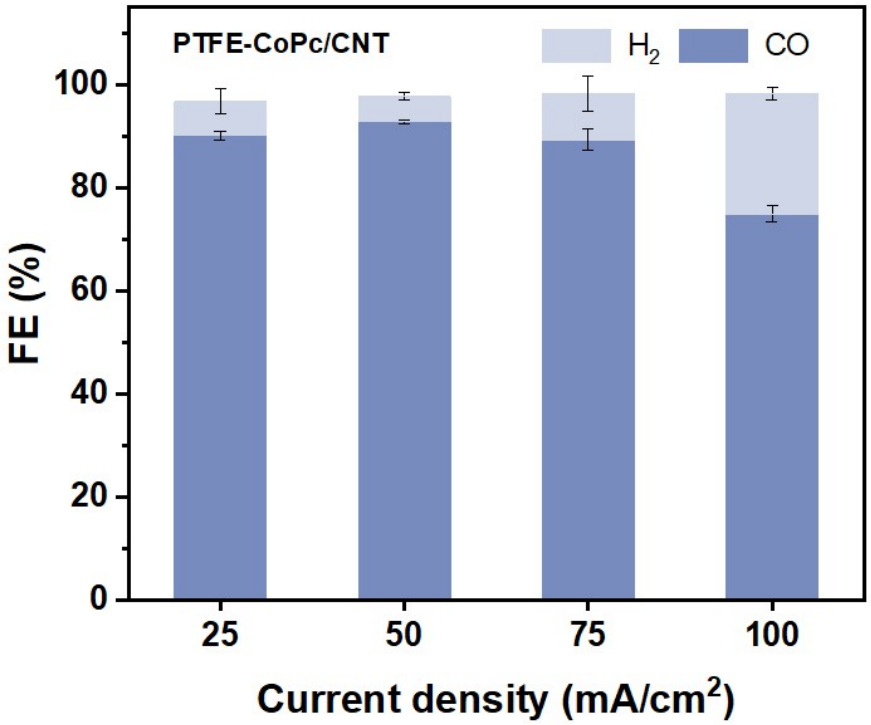


**Figure S17** FE of $CO_2RR$ for PTFE-CoPc/CNT in a MEA. The $CO_2RR$ performance of PTFE-CoPc/CNT started to decline from 50 mA/cm$^2$, and $FE_{CO}$ remained above 75% in the current range of 0-100 mA/cm$^2$. The overall FEs were around 100%.

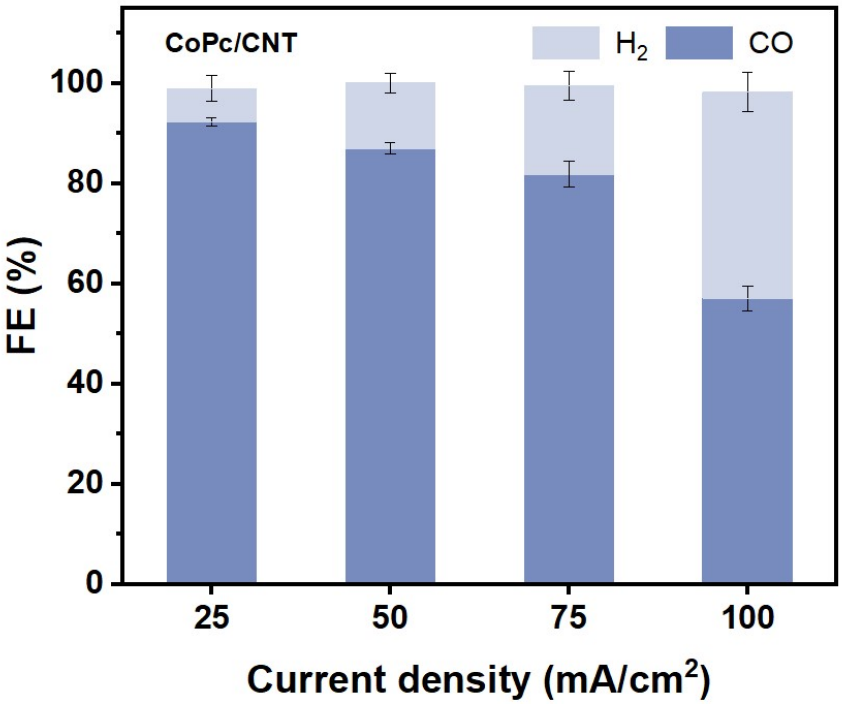


**Figure S18** FE of $CO_2RR$ for CoPc/CNT in a MEA. CoPc/CNT experienced a rapid deterioration as the current density increases, with $FE_{CO}$ of only 57% at 100 mA/cm$^2$. The overall FEs were around 100%.

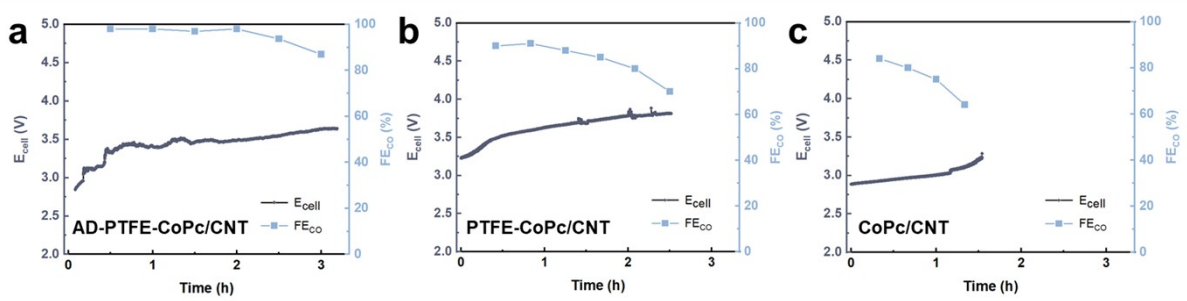


**Figure S19** Long-term durability of (a) AD-PTFE-CoPc/CNT, (b) PTFE-CoPc/CNT and (c) CoPc/CNT in the MEA device at a total current of 0.3 A.

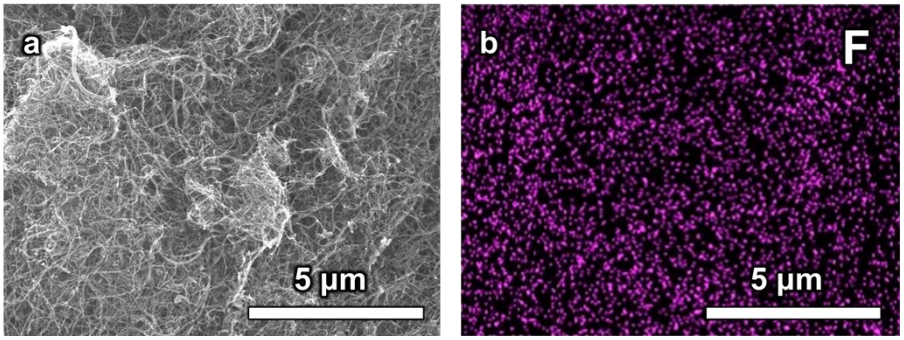


**Figure S20** (a) SEM and (b) EDS elemental mapping images of AD-PTFE-CoPc/CNT after $CO_2$RR. The F element remained well-dispersed.

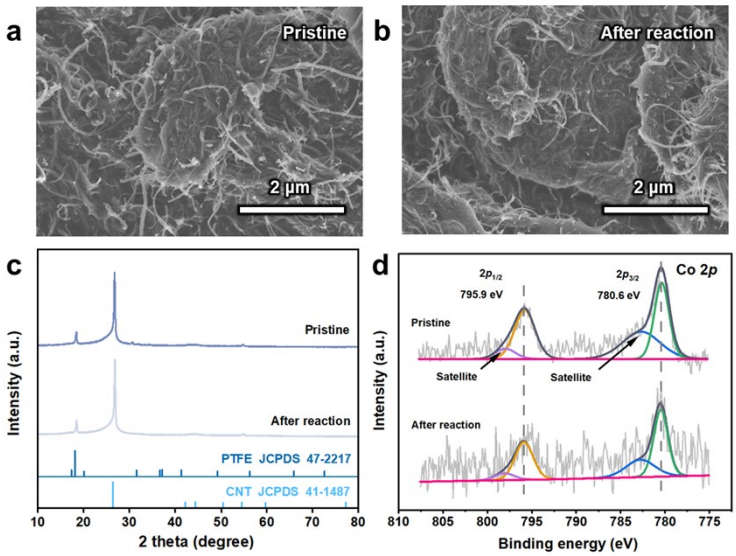


**Figure S21** SEM images of the electrode loaded with AD-PTFE-CoPc/CNT (a) in pristine state, (b) after reaction. (c) XRD patterns and (d) Co 2p XPS spectra of the electrode loaded with AD-PTFE-CoPc/CNT in pristine state and after reaction.

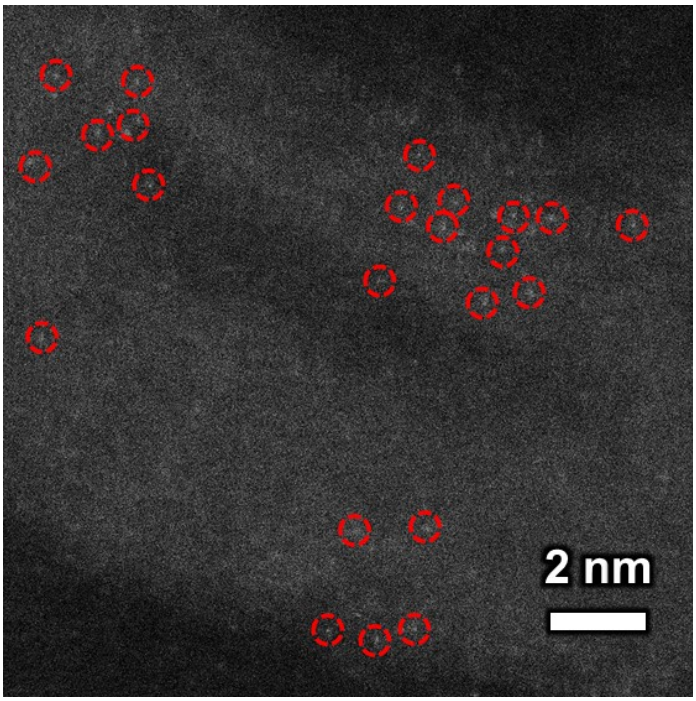


**Figure S22** AC-TEM image of AD-PTFE-CoPc/CNT after $CO_2$RR.

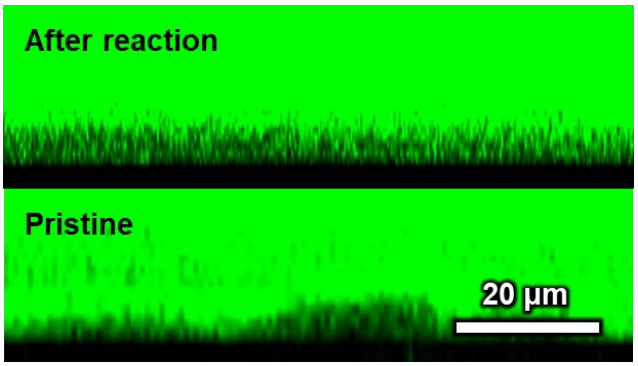


**Figure S23** Cross-section fluorescence images of the electrode coated with AD-PTFE-CoPc/CNT before and after the $CO_2$RR.

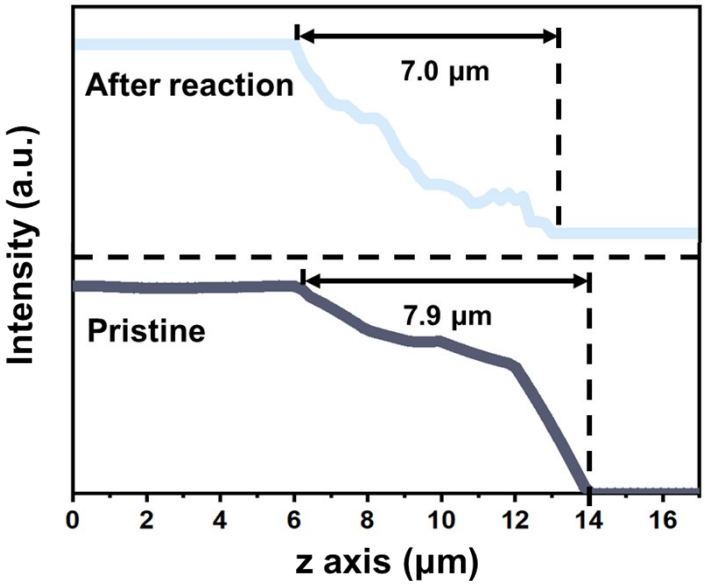


**Figure S24** Corresponding z axis fluorescence intensity line scans of the electrode coated with AD-PTFE-CoPc/CNT before and after the $CO_2$RR.

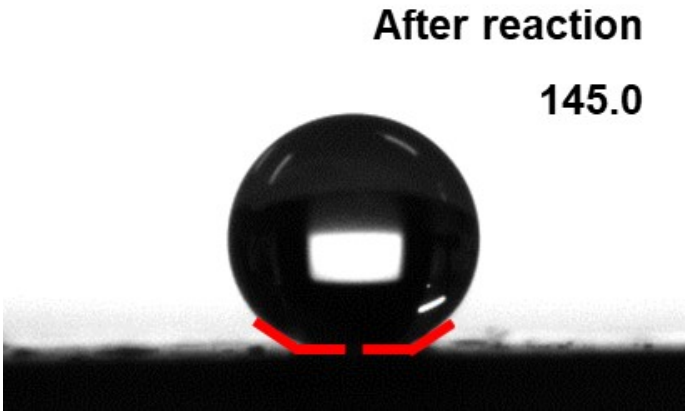


**Figure S25** Contact angle of the electrode coated with AD-PTFE-CoPc/CNT after $CO_2$RR.

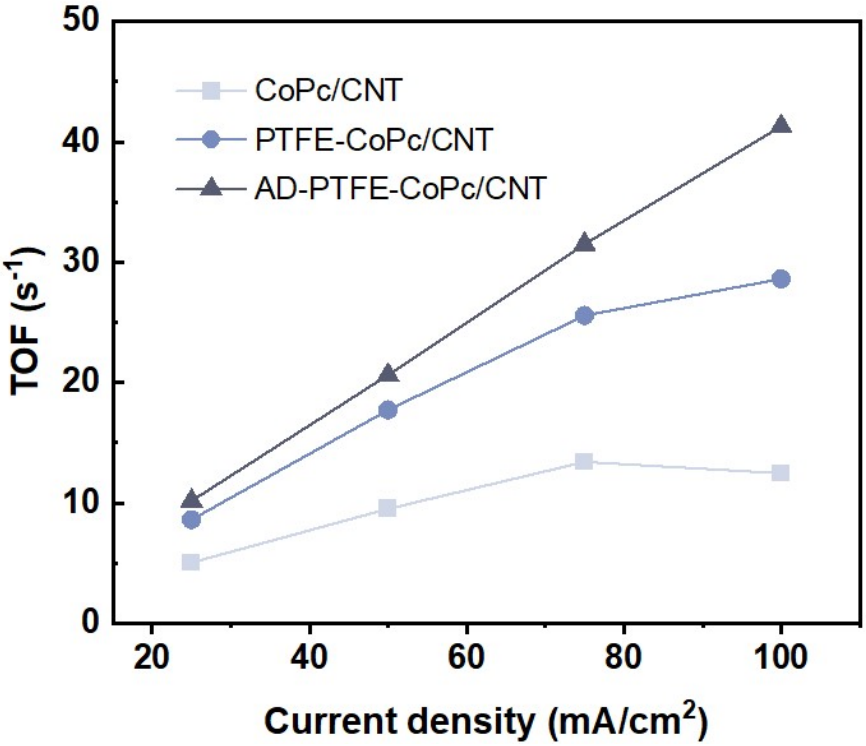


**Figure S26** TOF of $CO_2$RR for CoPc/CNT, PTFE-CoPc/CNT, and AD-PTFE-CoPc/CNT in a MEA. AD-PTFE-CoPc/CNT demonstrated the highest catalyst activity.

**Table S1** ICP-OES results of CoPc/CNT, PTFE- CoPc/CNT and AD-PTFE- CoPc/CNT

| Sample | Co Content (wt %) | CoPc Content (wt %) |
|---|---|---|
| CoPc/CNT | 0.14 | 1.18 |
| PTFE-CoPc/CNT | 0.08 | 0.67 |
| AD-PTFE-CoPc/CNT | 0.07 | 0.59 |

**Table S2** Fitted values of the component parameters obtained by modeling the impedance of the GDE using a ladder circuit

| Components | CoPc/CNT | Error (±) | PTFE-CoPc/CNT | Error (±) | AD-PTFE-CoPc/CNT | Error (±) |
|---|---|---|---|---|---|---|
| $R_s$ ($\Omega \cdot cm^2$) | 3.47 | 0.018 (0.5%) | 3.04 | 0.018 (0.6%) | 4.11 | 0.054 (1.3%) |
| $C_{trap}$ (F) | 0.00936 | 0.000029 (3.1%) | 0.000924 | 0.000022 (2.4%) | 0.000192 | 0.000018 (9.5%) |
| $C_{dl}$ (F) | 0.00188 | 0.00015 (7.9%) | 0.00120 | 0.000057 (4.7%) | 0.000856 | 0.000036 (4.2%) |
| $C_d$ (F) | 0.130 | 0.0081 (6.3%) | 0.0476 | 0.0044 (9.3%) | 0.00461 | 0.00049 (10.6%) |
| $R_d$ ($\Omega \cdot cm^2$) | 2.71 | 0.091 (3.4%) | 5.10 | 0.24 (4.8%) | 5.94 | 0.31 (5.3%) |
| $R_{ct}$ ($\Omega \cdot cm^2$) | 4.25 | 0.20 (4.6%) | 12.1 | 0.33 (2.8%) | 6.96 | 0.27 (3.9%) |
| $R_{trns}$ ($\Omega \cdot cm^2$) | 3.35 | 0.20 (5.9%) | 5.52 | 0.34 (6.2%) | 1.80 | 0.090 (5.0%) |

**Table S3** $CO_2RR$ performance comparison of state-of-the-art molecular catalysts

| Materials | Current density | $FE_{CO}$ | TOF | Reactor | Reference |
|---|---|---|---|---|---|
| AD-PTFE-CoPc/CNT | 200 mA/cm$^2$ | 85% | 74.3 s$^{-1}$ | Flow cell | This work |
| AD-PTFE-CoPc/CNT | 100 mA/cm$^2$ | 95% | 41.3 s$^{-1}$ | Flow cell | This work |
| 700 °C CoPC/C | 40 mA/cm$^2$ | 85% | 1.1 s$^{-1}$ | Flow cell | ACS Catal. 2022, 12, 14571 |
| CoPc-2$H_2$Por | 25 mA/cm$^2$ | 78% | 0.23 s$^{-1}$ | Flow cell | Adv. Mater. 2022, 34, 2203139 |
| N-CoMe$_2$Pc/NRGO (6:10) | 90 mA/cm$^2$ | 80% | 8.4 s$^{-1}$ | Flow cell | Chem. Eng. J. 2022, 15, 133050 |
| CuPcF$_8$-CoNPc-COF | 25.7 mA/cm$^2$ | 97% | 2.87 s$^{-1}$ | Flow cell | J. Am. Chem. Soc. 2021, 143, 18052 |
| CNT@CMP(CoPc-H2Pc) | 150 mA/cm$^2$ | 81% | 2.5 s$^{-1}$ | Flow cell | Angew.Chem. Int. Ed. 2021, 61, e202115503 |
| CoPc-EA-COF | 37 mA/cm$^2$ | 86% | 0.58 s$^{-1}$ | Flow cell | Chem. Eng. J. 2024, 488, 150812 |
| CoPc/CNT-AG | 200 mA/cm$^2$ | 95% | 83.9 s$^{-1}$ | Flow cell | Adv. Funct. Mater. 2022, 32, 2107301 |
| CoPc–Cu–O | 17.3 mA/cm$^2$ | 85% | 0.63 s$^{-1}$ | Flow cell | ACS Catal. 2020, 10, 4326 |
| NiPc-OMe MDE | 150 mA/cm$^2$ | 95% | 12 s$^{-1}$ | Flow cell | Nat. Energy 2020, 5, 684 |
| Co(PyPc) | 100 mA/cm$^2$ | 95% | 6.4 s$^{-1}$ | Flow cell | Sci. adv. 2023, 9, eadh9986 |
| CoPc@NU-1000-$\hbar$ | 1.5 mA/cm$^2$ | 80% | 0.12 s$^{-1}$ | Flow cell | Angew.Chem. Int. Ed. 2023, 62, e202219046 |
| CoPc-PI-COF-1 | 22.3 mA/cm$^2$ | 95% | 2.2 s$^{-1}$ | Flow cell | J. Am. Chem. Soc. 2021, 143, 7104 |
| CoPc/Mg(OH)$_2$/NC | 100 mA/cm$^2$ | 95% | 7.0 s$^{-1}$ | Flow cell | Adv. Funct. Mater. 2023, 33, 2214609 |
| EtO$_8$–CoPc\|CNP | 300 mA/cm$^2$ | 93% | 149.3 s$^{-1}$ | Flow cell | J. Am. Chem. Soc. 2023, 145, 4414 |
| CoPc-PI-COF-3 | 45 mA/cm$^2$ | 88% | 0.6 s$^{-1}$ | Flow cell | Angew.Chem. Int. Ed. 2022, 61, e202114244 |
| CoPc/$C_3N_4$/G | 67.8 mA/cm$^2$ | ~100% | 50.5 s$^{-1}$ | Flow cell | ACS Catal. 2024, 14, 8138 |
| CoPc-Py-CNT | 69.5 mA/cm$^2$ | 94% | 3.65 s$^{-1}$ | Flow cell | Chem. Eng. J. 2023, 465, 142858 |
| CoPc/GDY/G | 100 mA/cm$^2$ | 97% | 37 s$^{-1}$ | Flow cell | J. Am. Chem. Soc. 2021, 143, 8679 |